

# Multifaceted Characterization And In Vitro Assessment Of Polyurethane-Based Electrospun Fibrous Composite For Bone Tissue Engineering

This article was published in the following Dove Press journal:  
*International Journal of Nanomedicine*

Haoli Jiang<sup>1</sup>  
Mohan Prasath Mani<sup>2</sup>  
Saravana Kumar  
Jaganathan<sup>3-6</sup>

<sup>1</sup>Orthopaedics Department, The Third People's Hospital of Shenzhen, Shenzhen, Guangdong 518114, People's Republic of China; <sup>2</sup>School of Biomedical Engineering and Health Sciences, Faculty of Engineering, Universiti Teknologi Malaysia, Skudai 81310, Malaysia;

<sup>3</sup>Department for Management of Science and Technology Development, Ton Duc Thang University, Ho Chi Minh City, Vietnam; <sup>4</sup>Faculty of Applied Sciences, Ton Duc Thang University, Ho Chi Minh City, Vietnam; <sup>5</sup>IJNUTM Cardiovascular Engineering Center, School of Biomedical Engineering and Health Sciences, Faculty of Engineering, Universiti Teknologi Malaysia, Skudai 81310, Malaysia;

<sup>6</sup>Department of Engineering, Faculty of Science and Engineering, University of Hull, Hull HU6 7RX, UK

**Introduction:** Recently several new approaches were emerging in bone tissue engineering to develop a substitute for remodelling the damaged tissue. In order to resemble the native extracellular matrix (ECM) of the human tissue, the bone scaffolds must possess necessary requirements like large surface area, interconnected pores and sufficient mechanical strength.

**Materials and methods:** A novel bone scaffold has been developed using polyurethane (PE) added with wintergreen (WG) and titanium dioxide (TiO<sub>2</sub>). The developed nanocomposites were characterized through field emission scanning electron microscopy (FESEM), Fourier transform and infrared spectroscopy (FTIR), X-ray diffraction (XRD), contact angle measurement, thermogravimetric analysis (TGA), atomic force microscopy (AFM) and tensile testing. Furthermore, anticoagulant assays, cell viability analysis and calcium deposition were used to investigate the biological properties of the prepared hybrid nanocomposites.

**Results:** FESEM depicted the reduced fibre diameter for the electrospun PE/WG and PE/WG/TiO<sub>2</sub> than the pristine PE. The addition of WG and TiO<sub>2</sub> resulted in the alteration in peak intensity of PE as revealed in the FTIR. Wettability measurements showed the PE/WG showed decreased wettability and the PE/WG/TiO<sub>2</sub> exhibited improved wettability than the pristine PE. TGA measurements showed the improved thermal behaviour for the PE with the addition of WG and TiO<sub>2</sub>. Surface analysis indicated that the composite has a smoother surface rather than the pristine PE. Further, the incorporation of WG and TiO<sub>2</sub> improved the anticoagulant nature of the pristine PE. In vitro cytotoxicity assay has been performed using fibroblast cells which revealed that the electrospun composites showed good cell attachment and proliferation after 5 days. Moreover, the bone apatite formation study revealed the enhanced deposition of calcium content in the fabricated composites than the pristine PE.

**Conclusion:** Fabricated nanocomposites rendered improved physico-chemical properties, biocompatibility and calcium deposition which are conducive for bone tissue engineering.

**Keywords:** polymer, TiO<sub>2</sub>/wintergreen, surface properties, apatite formation, tissue engineering

## Introduction

In bone tissue engineering, the several new promising approaches were emerging as a biological alternative for remodelling the damaged tissue. In designing bone scaffolds, several requirements are necessary such as large surface area, interconnected pores and sufficient mechanical strength in order to mimic the extracellular matrix (ECM) of the human tissue.<sup>1-3</sup> The fibres developed using polymeric structures can provide a large surface area with interconnected pores which can be utilized for various tissue engineering applications.<sup>4</sup> For the fabrication of fibres, various technologies were used such

Correspondence: Saravana Kumar Jaganathan  
Department for Management of Science and Technology Development, Ton Duc Thang University, Ho Chi Minh City, Vietnam  
Tel +84 28837755037  
Email saravana@tdtu.edu.vn

as drawing, self-assembly, phase separation, template synthesis, electrospinning, etc.,<sup>5</sup> Recently, the bone scaffold based on electrospinning technique has gained a great deal of attraction because of their structural similarity with the native bone extracellular matrix.<sup>6</sup> Electrospinning (ES) is the versatile and efficient technique used for making polymeric fibres with size ranging from micrometer to nanometer range. The physics behind the electrospinning technique is, when a high electric field is applied to the polymer solution leads to the formation of polymer jet. If the applied voltage overcomes the threshold value, it results in the fine fibres that deposited on the collector plate.<sup>7</sup>

Electrospinning is used to spin nano-fibrous structures from natural to synthetic polymers. The natural polymers like collagen, chitosan and silk fibroin whereas synthetic polymers like poly(L-lactide) (PLA), polycaprolactone (PCL) and polyurethane are electrospun widely.<sup>3</sup> For the last few years, this technique was found to be widespread in biomedical applications such as drug delivery, wound dressing, tissue engineering scaffolds and also in medical implants.<sup>8–13</sup> In this research, the bone scaffold was fabricated using polyurethane as a matrix via electrospinning. It was selected because of their excellent oxidative stability and biodegradability behaviour.<sup>14,15</sup> Owing to their desirable characteristics, the electrospun polyurethane fibres were widely used in various biomedical applications such as tissue engineering of skin, bone and graft.<sup>16–18</sup> The most important strategy in the designing of the bone scaffold is it should promote cell attachment for osteogenic differentiation and also have sufficient mechanical strength to support the new bone tissue.<sup>19</sup> Various types of approaches have been explored in the bone tissue engineering for the past few years to improve the significant parameters like cellular response and their mechanical strength.<sup>20</sup> Unnithan et al blended emu oil into PE and observed that the fabricated composite membranes enhanced cell adhesion and proliferation.<sup>16</sup> In another study, Jaganathan et al fabricated electrospun PE composite mixed with neem oil and sunflower which showed improved cellular response and suggested it as a suitable candidate for bone tissue engineering.<sup>21</sup> These works of literature showed that the essential oil plays a vital role in influencing the cellular response. Silva et al fabricated electrospun alginate nanofibrous loaded with magnesium oxide and observed the improvement in the tensile strength.<sup>22</sup> Tobias et al electrospun poly(D,L-lactide) (PLA) mat decorated with zinc oxide (ZnO) and it was reported to possess improved mechanical strength.<sup>23</sup> Hence, it was evident that the metallic particles play an important role in influencing the

mechanical strength of the composites. In this research, wintergreen (WG) oil and titanium dioxide (TiO<sub>2</sub>) were selected.

The use of oils is widely practiced in traditional treatments to alleviate the bone-related pain. Usually, the essential oils obtained from plants possess medicinal properties like anti-inflammatory, antiseptic and antispasmodic.<sup>24</sup> These properties would help in reducing the pain created in muscle and joint. *G. procumbens* belongs to the Ericaceae family which is an evergreen shrub and widely found in the eastern parts of North America.<sup>25</sup> The essential oil based on wintergreen is reported to rich in methyl salicylate used for flavouring candies, chewing gums, mouthwashes and toothpaste.<sup>26</sup> It is also used in clinical applications for the treatment of cellulites.<sup>27</sup> The chemical components of WG are limonene,  $\beta$ -pinene,  $\alpha$ -pinene, sabinene, myrcene, fenchone, menthone and methyl salicylate.<sup>25</sup> Moreover, this essential oil was reported to possess moderate antibio-film, antimicrobial, antioxidant and antiradical activity.<sup>25</sup> Tissue engineering scaffolds added with TiO<sub>2</sub> showed to be improved biological responses. Wang et al studied the osteogenic potential of electrospun poly(vinyl pyrrolidone)-titania-silica (PVP-TiO<sub>2</sub>-SiO<sub>2</sub>) nanofibres. The results indicated that the PVP-TiO<sub>2</sub>-SiO<sub>2</sub> nanofibre meshes influenced the osteogenic potential.<sup>28</sup> Adhikari et al developed electrospun porous TiO<sub>2</sub> nanofibres for bone tissue engineering and observed that the porous TiO<sub>2</sub> nanofibres showed improved biocompatibility for bone regeneration compared to the other non-porous TiO<sub>2</sub>.<sup>29</sup> Hence, these studies motivated us to use TiO<sub>2</sub> in this research. The scope of this work is to generate and test the electrospun bone scaffold based on polyurethane decorated with TiO<sub>2</sub> and WG oil.

## Materials And Methods

### Materials

Tecoflex EG-80A (polyether medical-grade polyurethane) was supplied by Lubrizol, Wickliffe, OH, USA. PE was dissolved using dimethylformamide (DMF) solvent obtained from Merck, Burlington, NJ, USA. WG oil was purchased locally market AEON, Johor, Malaysia, while TiO<sub>2</sub> was supplied from Sigma Aldrich, Gillingham, UK. The reagents used for coagulation study were procured from Diagnostic Enterprise, Thiruvananthapuram, India.

### Preparation Of Polymer Solution

PE in DMF solution was prepared at 9 wt% and stirring for 12 hrs at room temperature for a homogenous solution. Aqueous WG solution was prepared at 4 v/v% by adding

120  $\mu\text{L}$  in 3 mL of DMF and stirred for 1 hr at room temperature. Similarly, 4 wt% of colloidal  $\text{TiO}_2$  solution was obtained by adding 0.120 g in 3 mL of DMF and stirred for 1 hr at room temperature, respectively. Finally, the prepared WG and  $\text{TiO}_2$  solution was added to PE solution to make PE/WG (8:1 (v/v%)) and PE/WG/ $\text{TiO}_2$  (8:0.5:0.5 (v/v%)) respectively.

## Electrospinning Process

PE solutions and its suspensions were converted into fibrous scaffold using electrospinning technique. The prepared solution was electrospun at constant processing conditions with an applied voltage of 11.5 kV, collection distance of 20 cm and a flow rate of 0.3 mL/hr, respectively. The electrospun fibres were collected using aluminium foil and vacuum dried to remove any residues present in the fabricated membranes.

## Nanofibre Characterizations

### Field Emission Scanning Electron Microscopy Analysis

The fibre morphology of the electrospun membranes was examined through FESEM unit (Hitachi SU8020, Tokyo, Japan). A small piece of electrospun membranes was gold plated at 20 mA for 2 mins and imaged at different magnifications. The average fibre diameter was computed (Image J software) using those images.

### Fourier Transform Infrared Spectroscopy Analysis

The infrared (IR) spectrum of electrospun samples was measured in Nicolet iS 5, Thermo Fischer Scientific, Waltham, MA, USA. The attenuated total reflection (ATR) crystal employed is Zinc Selenium ( $\text{ZnSe}$ ). The wavelengths for the electrospun samples were recorded between 600 and 4000  $\text{cm}^{-1}$  at 4  $\text{cm}^{-1}$  resolution.

### Contact Angle Measurements

Contact angle measurements were performed using a video contact angle (VCA) contact angle unit (AST products, Inc., Billerica, MA, USA). This was done by placing a droplet of water on the surface and immediately an image was captured using a video camera. From the captured image, the contact angle was measured using computer integrated software.

### X-Ray Diffraction (XRD) Analysis

The phase and structure of the electrospun nanofibres were evaluated using XRD analysis. The XRD pattern of the electrospun membranes was recorded in XRD diffractometer

(Rigaku, Tokyo, Japan) having  $\text{CuK}\alpha$  radiation and the angle was recorded between  $10^\circ$  and  $90^\circ$ .

## Atomic Force Microscopy (AFM) Analysis

Surface roughness was measured using AFM unit (NanoWizard<sup>®</sup>, JPK Instruments, Berlin, Germany) in a normal atmosphere. A small piece of electrospun membranes was scanned in tapping mode with size area of  $20\text{ }\mu\text{m} \times 20\text{ }\mu\text{m}$  and the high-quality images were obtained in 256 resolution.

## Thermal Analysis

The thermal behaviour of electrospun membranes was determined through thermogravimetric analysis (TGA) unit (PerkinElmer, Waltham, MA, USA) in a nitrogen atmosphere. For testing, 3 mg of sample was used and the heating was done at a rate of  $10^\circ/\text{min}$  with the temperature between  $30^\circ\text{C}$  to  $1000^\circ\text{C}$  respectively.

## Tensile Testing

The tensile strength of electrospun scaffolds was calculated from stress-strain plots recorded using uniaxial tester (Gotech Testing Machines, AI-3000). The samples with a size of  $40\text{ mm} \times 15\text{ mm}$  were clamped in the uniaxial tester and the gauge length, load cell and strain rate were 20 mm, 500 N and 10 mm/min, respectively. The average tensile strength was computed and expressed in MPa.

## Coagulation Assays

### Prothrombin Test (PT)

The measurement of PT determines the extrinsic pathway of the electrospun membranes. To start the assay, a small piece of the sample was preincubated with 50  $\mu\text{L}$  of platelet-poor plasma (PPP) at  $37^\circ\text{C}$ . After, it was added with 50  $\mu\text{L}$  of sodium chloride ( $\text{NaCl}$ )-thromboplastin (factor III) containing calcium ( $\text{Ca}^{2+}$ ) ions. Finally, the time for blood clot formation was determined with the aid of stopwatch and a steel hook.

### Activated Partial Thromboplastin Time (APTT)

The measurement of APTT determines the intrinsic pathway of the electrospun membranes. First, a small piece of the sample was incubated with 50  $\mu\text{L}$  of PPP at  $37^\circ\text{C}$ . Then, it was added with 50  $\mu\text{L}$  of rabbit brain encephalin followed by adding 50  $\mu\text{L}$  of calcium chloride ( $\text{CaCl}_2$ ) (0.025 M). Finally, the time for blood clot formation was determined with the aid of stopwatch and a steel hook.

## Haemolysis Test

To begin the assay, the samples were cut into small size and equilibrated with physiologic saline at 37°C for 30 mins. Then, the equilibrated samples were incubated with a mixture of aliquots of citrated blood and diluted saline (4:5 (v/v %)) for 60 mins at 37°C. After incubation, the mixtures were taken out and centrifuged at 3000 rpm for 5 mins. Finally, the optical density (OD) was recorded at 542 nm for the aspirated supernatant which indicates the release of haemoglobin. The percentage of haemolysis or haemolytic index was calculated using the formula:

$$\text{Haemolysis ratio (HR)} = (\text{TS} - \text{NC}) / (\text{PC} - \text{NC}) \times 100\%$$

where TS, NC and PC are measured absorbance values of the test sample, negative control and positive control at 542 nm, respectively.

## Bioactivity Test

The bioactivity test was performed by soaking the electrospun fibres in simulated body fluid (SBF). The electrospun fibres of  $1 \times 1 \text{ cm}^2$  were left in  $1.5 \times \text{SBF}$  (pH 7.4; 37°C) for 14 days. After 14 days, the samples were cleaned, dried and imaged using scanning electron microscopy (SEM) (Hitachi Tabletop TM3000, Tokyo, Japan) equipped with energy dispersive X-ray analyser (EDX) to evaluate the amount of calcium deposition.

## Cytocompatibility Assay

3-(4,5-dimethylthiazol-2-yl)-5-(3-carboxymethoxyphenyl)-2-(4-sulfophenyl)-2H tetrazolium, inner salt (MTS) assay was used to determine the cell viability of the electrospun scaffolds. The assay was done using fibroblast cells (Human Skin Fibroblast Cells 1184, ECACC, UK, primary cells obtained from the dermis of the skin) grown in Dulbecco's modified Eagle's medium added with 10% (v/v) fetal bovine serum and maintained at 37°C and 5% CO<sub>2</sub>. Before seeding, the scaffold was cut into small size and placed in 96 well plates. After this,  $10 \times 10^3$  cells/cm<sup>2</sup> were seeded onto the scaffolds in each well and cultured for 5 days. After 5 days, the medium was added with 20% of MTS solution and further incubated for 4 hrs. Afterwards, OD was determined at 490 nm using microplate reader to determine the cell viability.

## Statistical Analysis

All biological experiments were performed three times separately. The statistical significance ( $p < 0.05$ ) was calculated

using one way ANOVA followed by Dunnett post hoc test and expressed as mean  $\pm$  SD.

# Result And Discussion

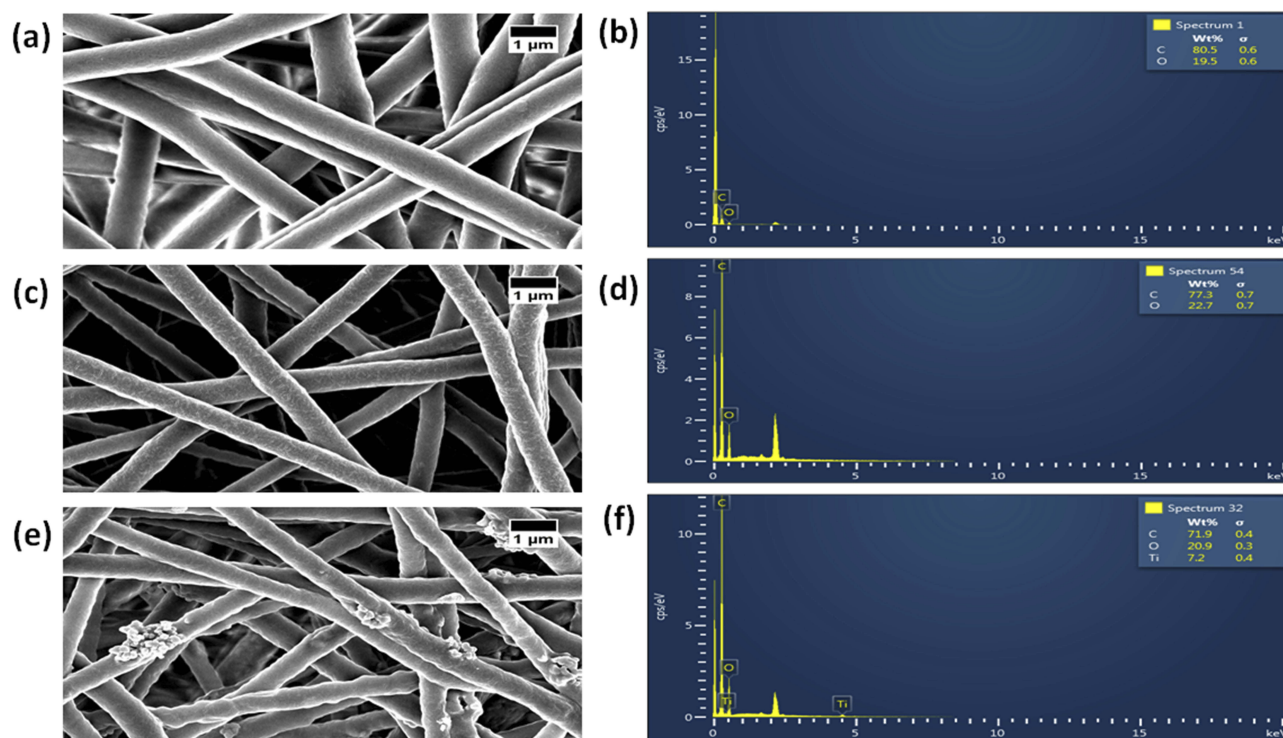
## FESEM Analysis

Figure 1 depicts the FESEM images of electrospun PE, PE/WG and PE/WG/TiO<sub>2</sub> nanocomposites. From the figure, it observed that the electrospun PE and their nanocomposites had smooth fibres with beadless structure. The average fibre diameters of PE, PE/WG and PE/WG/TiO<sub>2</sub> nanocomposites were reported to be  $894 \pm 151 \text{ nm}$ ,  $664 \pm 150 \text{ nm}$  and  $566 \pm 145 \text{ nm}$ , respectively. The fibre diameter results using Image J indicated that the PE/WG and PE/WG/TiO<sub>2</sub> nanocomposites had reduced fibre diameter than the pure PE. The decrease in the fibre diameter was due to the addition of WG and TiO<sub>2</sub> into the polyurethane matrix. This behaviour was attributed to the added constituents which had influenced the properties of electrospun solution. The added constituents influenced the viscosity which eventually led to the reduction of fibre diameter.<sup>30</sup> In a recent study, it was reported that the decrease in polymer concentration had reduced the fibre diameter.<sup>31</sup> In this study, there is a decrease in polymer concentration while adding WG and TiO<sub>2</sub> which would have also contributed to the reduction of fibre diameter of the composites. Linh et al observed that the smaller fibre diameter will be conducive for improved osteoblast cell response.<sup>3</sup> The reduced fibre diameter of electrospun nanocomposites will be conducive for new bone tissue growth. Further EDX confirmed the presence of titanium (7.2%) in the polyurethane matrix as shown in Figure 1.

## FTIR Analysis

The characteristic peaks of the electrospun PE, PE/WG, PE/WG/TiO<sub>2</sub> are depicted in Figure 2. The absorption band of PE showed a broad band at  $3323 \text{ cm}^{-1}$  signals the NH group and its vibrations at  $1597 \text{ cm}^{-1}$  and  $1531 \text{ cm}^{-1}$ . A sharp peak is shown at  $2940 \text{ cm}^{-1}$ , and  $2854 \text{ cm}^{-1}$  denotes the CH stretching and its vibrations were seen at  $1414 \text{ cm}^{-1}$ . The carboxylic C=O stretching is reflected as twin peaks at  $1702 \text{ cm}^{-1}$  and  $1730 \text{ cm}^{-1}$ , respectively. Further, there were other peaks present between  $500 \text{ cm}^{-1}$  and  $1200 \text{ cm}^{-1}$  region. The peaks  $770 \text{ cm}^{-1}$ ,  $1105 \text{ cm}^{-1}$  and  $1220 \text{ cm}^{-1}$  corresponds to C-O-C and C-OH group, respectively.<sup>32,33</sup> From the IR spectrum of electrospun PE/WG and PE/WG/TiO<sub>2</sub>





**Figure 1** FESEM images and EDX of (A, B) PE, (C, D) PE/WG and (E, F) PE/WG/TiO<sub>2</sub>. Sample with size of 1 cm \* 1 cm was cut and imaged in Hitachi SU8020 at different magnifications.

nanocomposites, it was observed no additional peaks were formed but the intensity of the absorption bands was increased with the addition of WG and TiO<sub>2</sub>. The increase in intensity was because of hydrogen bond formation between the molecules of WG and TiO<sub>2</sub> with the PE molecules.<sup>16</sup> The formation of hydrogen bond confirms the presence of WG and TiO<sub>2</sub> in the PE matrix.

## Wettability Measurements

The contact angle measurements of electrospun PE, PE/WG and PE/WG/TiO<sub>2</sub> membranes were presented. It revealed that the contact angle of PE/WG and PE/WG/TiO<sub>2</sub> was increased compared to pure PE. The contact angle of PE was found to be  $106 \pm 2.517^\circ$  whereas the contact angle of PE/WG and PE/WG/TiO<sub>2</sub> was observed to be  $112 \pm 0.5774^\circ$  and  $119 \pm 0.5774^\circ$ , respectively. The

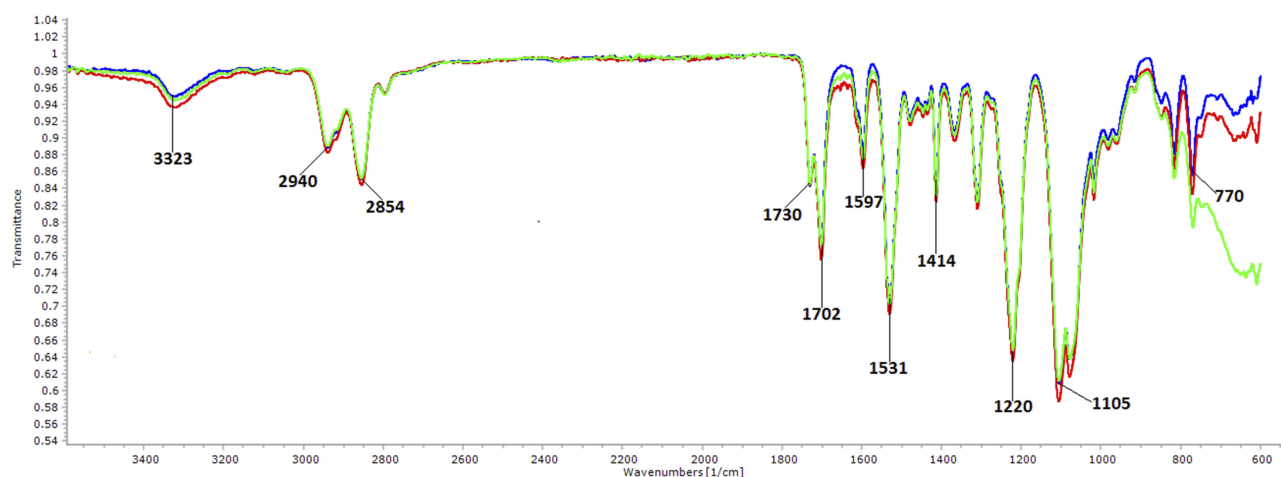


**Figure 2** FTIR of PE (blue line), PE/WG (red line) and PE/WG/TiO<sub>2</sub> (green line). Sample with size of 1 cm \* 1 cm was cut and measured in wavelength range between 600 and 4000 cm<sup>-1</sup> in Nicolet iS5.

experimental results clearly showed that the addition of WG and  $\text{TiO}_2$  into the PE matrix decreased the wettability of the PE membrane. Jaganathan et al electrospun polyurethane scaffold mixed with carotino oil. It was depicted that the contact angle of PE was increased with the addition of carotino oil and concluded the reason for this behaviour was due to their smaller fibre diameter.<sup>32</sup> Hence, in this study, the fabricated composites showed a smaller fibre diameter which would have resulted in the decreased wettability behaviour. It has been reported that the hydrophobic surface would facilitate the healing of bone defects through absorption of more amount of proteins.<sup>33</sup> Hence, the hydrophobic surface of the newly fabricated electrospun nanocomposites will favour the enhanced absorption of proteins for the healing of bone defects.

## XRD Analysis

XRD pattern was obtained for the as-spun membranes to determine the crystallinity of the membranes as indicated in Figure 3. A broad peak showed at  $20^\circ$  in the pristine PE indicates their amorphous behaviour. In the case of PE/WG, it has only broad peak as that of PE membrane without any additional peaks observed. For the PE/WG/ $\text{TiO}_2$ , multiple peaks at  $25.270^\circ$ ,  $36.910^\circ$ ,  $37.771^\circ$ ,  $38.528^\circ$ ,  $48.010^\circ$ ,  $53.849^\circ$ ,  $55.037^\circ$ ,  $62.073^\circ$ ,  $62.649^\circ$  in addition to the broad peak at  $20^\circ$ . The peaks shown correlate with the planes of titanium as reported in previous studies.<sup>34</sup>

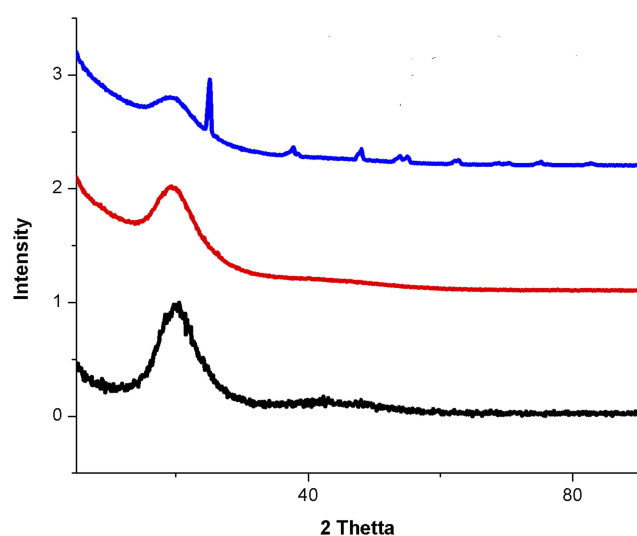


**Figure 3** XRD images of a) PE (black line), b) PE/WG (red line) and c) PE/WG/ $\text{TiO}_2$  (blue line). Sample with size of  $1\text{ cm} \times 1\text{ cm}$  was cut and recorded in Rigaku having  $\text{CuK}\alpha$  radiation in angle between  $10^\circ$  and  $90^\circ$ .

Hence, the addition of  $\text{TiO}_2$  favoured the change in crystalline behaviour of the pristine PE.

## TGA Analysis

TGA assists the evidence for chemical interactions of PE with the WG and  $\text{TiO}_2$  and also to evaluate the thermal degradation behaviour. The experiment results of the thermal analysis are presented in Figure 4A. The results clearly showed that the fabricated nanocomposites displayed enhanced initial degradation temperature than the pristine PE indicating their higher thermal stability. The electrospun PE/WG and PE/WG/ $\text{TiO}_2$  nanofibres showed initial onset temperature of  $289^\circ\text{C}$  and  $280^\circ\text{C}$ , whereas the onset temperature for pure PE was found to be only  $266^\circ\text{C}$ . The weight loss curves of the electrospun nanofibres were depicted in Figure 4B and the number of weight loss peaks are shown in Table 1. It was evident that the number of peak weight loss was reduced in PE/WG and PE/WG/ $\text{TiO}_2$  compared to the pristine PE suggesting its increased thermal stability. Further, from Figure 4B, it can be inferred that the weight loss intensity of the PE was decreased with the addition of  $\text{TiO}_2$ .

## Mechanical Properties

The results of the mechanical properties of electrospun pure PE, PE/WG and PE/WG/ $\text{TiO}_2$  nanocomposites are indicated in Figure 5. The electrospun nanocomposites showed higher tensile strength than the pure PE nanofibres. The developed PE/WG and PE/WG/ $\text{TiO}_2$  nanocomposites showed an average tensile strength of 10.89 MPa and 13.85 MPa, while for PE, it was found to be 6.83 MPa, respectively. It was evident that the mechanical performance of PE was improved by blending WG and  $\text{TiO}_2$  nanofibres. The adhesion of fibres will form bonding between the polyurethane and molecules of WG resulting in the enhancement of the tensile strength which correlates with the findings of Unnithan et al.<sup>16</sup> They reported this behaviour to the adhesive property of emu oil. Jaganathan et al fabricated polyurethane/copper sulphate ( $\text{CuSO}_4$ ) scaffold using electrospinning. It was reported that the addition of copper sulphate resulted in the improvement of the tensile strength and attributed it to the smaller fibre diameter of the PE/ $\text{CuSO}_4$ .<sup>35</sup> Hence, the smaller diameter of the fabricated composites should have a role in influencing the tensile strength. Linh et al reported that the tensile strength of  $4.20 \pm 0.40$  suitable for bone tissue engineering.<sup>3</sup> Our measured tensile strength of the developed nanocomposites was found to be above reported

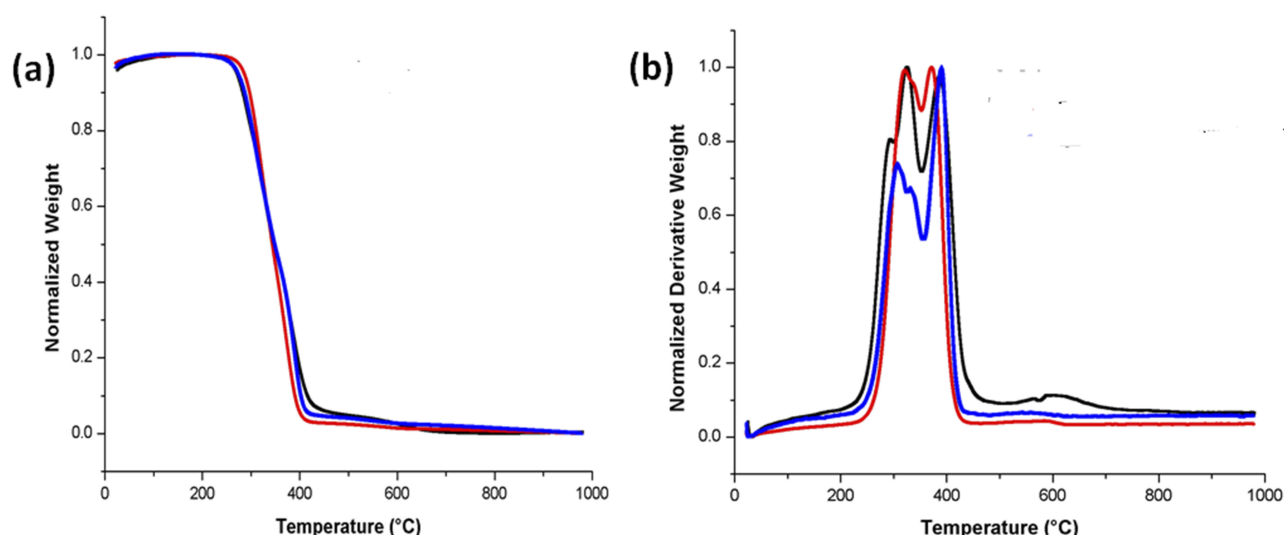


**Figure 4 (A)** TGA and **(B)** Weight residue of PE (black line), PE/WG (red line) and PE/WG/TiO<sub>2</sub> (blue line). Sample weighing 3 mg was heated between temperature range of 30-1000°C under nitrogen atmosphere in Perkin-Elmer TGA unit.

values indicating its appropriateness as a potential candidate for the bone tissue regeneration.

## AFM Analysis

The surface roughness of the electrospun pure PE, PE/WG and PE/WG/TiO<sub>2</sub> nanocomposites is measured using AFM analysis and their 3D images are denoted in Figure 6. The surface measurements depicted that the PE surface showed average roughness of 776 nm and for PE added with WG and WG/TiO<sub>2</sub>, it was found to be 474 nm and 554 nm, respectively. The results concluded that the PE surfaces were rougher while the incorporation of WG and TiO<sub>2</sub> resulted in the smoother surfaces. Jaganathan et al developed bone scaffold utilizing polyurethane added with corn and neem oil. It has been reported that the decrease in surface roughness of prepared composites was due to the added constituents.<sup>36</sup> In our study, a similar decrease in surface roughness was observed which is due to the presence of WG and titanium oxide in the polyurethane matrix. Kim et al reported that the scaffolds with smaller fibre showed a smoother surface compared to the larger

fibre diameter.<sup>37</sup> The smoothness of the fabricated composites is also due to their smaller fibre diameter. Ribeiro et al investigated the influence of surface roughness on osteoblast cell adhesion and proliferation in poly (L-lactide) (PLA) membranes. It was found that the fabricated membranes with smoother surfaces showed enhanced osteoblast cell response compared to the rougher surfaces.<sup>38</sup> Hence, our electrospun nanocomposites with smoother surfaces will facilitate osteoblast cell growth.

## Blood Compatibility Measurements

The antithrombogenic parameters of electrospun PE, PE/WG and PE/WG/TiO<sub>2</sub> determined via APTT and PT assay are presented in Figure 7A and B. It was found that the WG and TiO<sub>2</sub> incorporation increased the blood clotting time of the pristine PE. APTT assay displayed blood clotting time of the electrospun PE/WG and PE/WG/TiO<sub>2</sub> as  $180 \pm 5$  s and  $184 \pm 4$  s, and for pristine PE nanofibres, it was around  $162 \pm 2$  s. Similarly, PT assay displayed blood clotting time of electrospun PE/WG and PE/WG/TiO<sub>2</sub> about  $93 \pm 3$  s and  $97 \pm 2$  s, and for pristine PE nanofibres,

**Table 1** Weight Loss Peaks Of The Electrospun Membranes

Peaks	PE	PE/WG	PE/WG/TiO <sub>2</sub>
First weight loss peak	210°C to 302°C	229°C to 352°C	230°C to 325°C
Second weight loss peak	302°C to 353°C	352°C to 447°C.	325°C to 355°C
Third weight loss peak	353°C to 494°C	–	355°C to 461°C
Fourth weight loss peak	494°C to 760°C	–	–

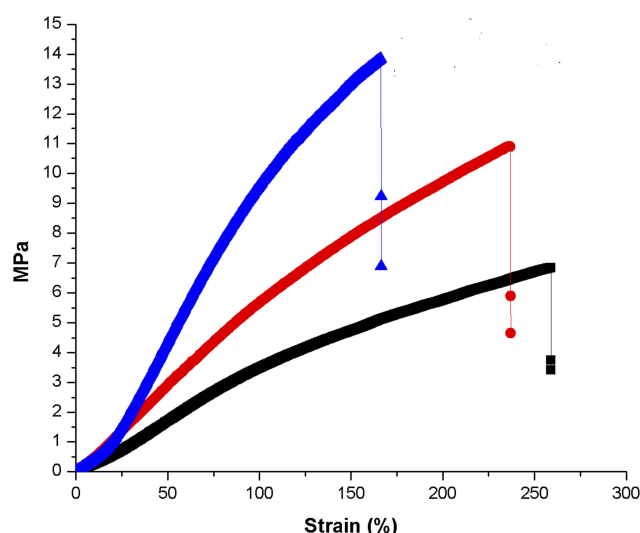


**Figure 5** Tensile strength of PE (black line), PE/WG (red line) and PE/WG/TiO<sub>2</sub> (blue line). Sample with size of 4 cm \* 1 0.5 cm was stretched at a cross head speed of 10 mm/min with a 500 N load cell in Gotech Testing Machines, AI-3000.

it was around  $85 \pm 1$  s. Further, haemolytic assay was performed to predict the safety of RBC with the electrospun membranes. The haemolysis results depicted that the developed nanocomposites were less toxic to the red blood cells (RBC). The value of the haemolytic index for the pristine PE nanofibres was 2.58%, and for the electrospun PE/WG and PE/WG/TiO<sub>2</sub>, it was only 1.56% and 1.68%, respectively, as shown in Figure 7c. According to ASTM F756-00(2000), the haemolytic index for the developed nanocomposites was less than 2% and it was a non-haemolytic material.<sup>32,33</sup> The blood compatibility is affected by several surface properties such as fibre diameter, wettability and surface roughness. Jaganathan et al prepared polyurethane/neem oil membranes and observed the increase in the blood clotting time than pure PE

because of an increase in surface roughness.<sup>39</sup> In another study, Jaganathan et al developed scaffold utilizing polyurethane added with sunflower and neem oil. It was shown that the addition of sunflower and neem oil resulted in the improvement of the blood compatibility behaviour and attributed this behaviour to their smaller fibre diameter and hydrophobic behaviour.<sup>21</sup> Hence, from this literature, it was shown that the blood compatibility was affected by smaller fibre diameter, hydrophobicity and increase in surface roughness. In this study, the addition of WG and titanium dioxide in PE matrix exhibited smaller fibre diameter and hydrophobicity which would have resulted in the improvement in the blood compatibility.

## Bone Mineralisation Testing

Bone mineralisation testing was performed to evaluate the amount of calcium deposition for the electrospun membranes. Figure 8 depicts the morphology and EDX graph of the electrospun scaffolds after 14 days in SBF. The progress of mineralization for the electrospun composites was higher (PE/WG- 102% and PE/WG/TiO<sub>2</sub> – 235%) than the pristine PE. The calcium deposition weight percentage for the pristine PE was reported to be 5.32% and for electrospun PE/WG and PE/WG/TiO<sub>2</sub> displayed calcium weight percentage of 10.73% and 17.84%, respectively. Hence, the addition of WG and TiO<sub>2</sub> increased the calcium deposition of the pristine PE insinuating its likely potential for bone tissue engineering.

## MTS Assay

The human dermal fibroblast (HDF) cell proliferation in the electrospun PE, PE/WG and PE/WG/TiO<sub>2</sub> is shown in

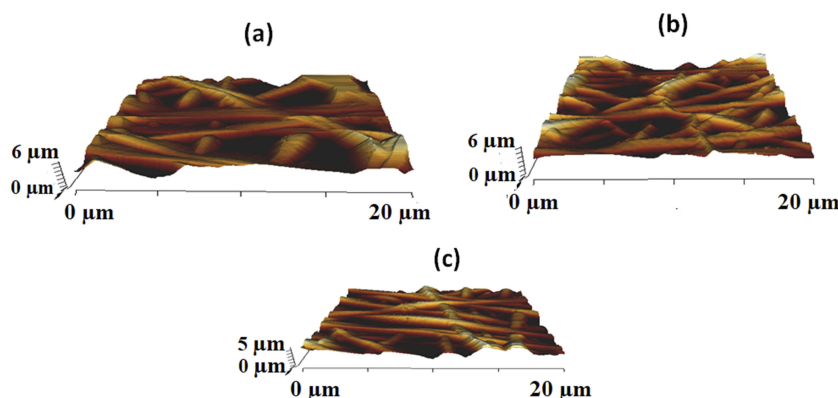


**Figure 6** AFM images of (A) PE, (B) PE/WG and (C) PE/WG/TiO<sub>2</sub>. Sample with size of 1 cm \* 1 cm was cut and scanned in 20 \* 20 μm size with 256 \* 256 pixels under normal atmosphere in Nanowizard, JPK instruments.



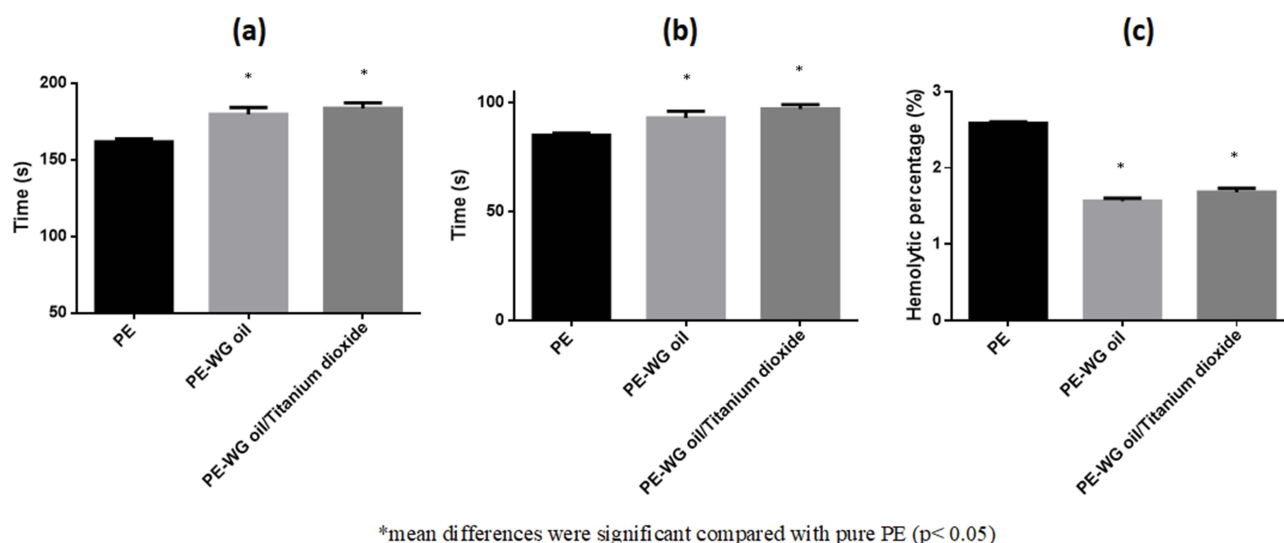


**Figure 7 (A)** APTT, **(B)** PT and **(C)** haemolytic assay of PE, PE/WG and PE/WG/TiO<sub>2</sub>. For APTT assay sample with size of 1 cm \* 1 cm was added with 50  $\mu$ L of platelet-poor plasma (PPP) followed by incubating with 50  $\mu$ L of reagent (rabbit brain cephaloplastin) and 50  $\mu$ L CaCl<sub>2</sub> (0.025 M) to calculate the blood clotting time. For PT assay sample with size of 1 cm \* 1 cm was added with 50  $\mu$ L of platelet-poor plasma (PPP) followed by incubating with 50  $\mu$ L of thromboplastin (Factor III) to calculate the blood clotting time. For haemolytic assay samples with size of 1 cm \* 1 cm added to the mixture of citrated blood and diluted saline (4:5 v/v%) for 1 hr at 37°C. After this, the samples were centrifuged and optical density (OD) was measured at 542 nm.

**Figure 9.** After 5 days cell culture, the HDF cells were more compatible with the electrospun membranes compared to the control. The pristine PE showed cell viability of  $130 \pm 4.348\%$ , while the electrospun PE/WG and PE/WG/TiO<sub>2</sub> scaffolds showed cell viability of  $131 \pm 11.49\%$  and  $138 \pm$

$2.106\%$ , respectively. The HDF cell proliferation rates for the developed nanocomposites were higher than pristine PE. The process of cell adhesion and proliferation to the scaffolds is multifactorial and it was influenced by various physico-chemical properties such as fibre diameter, wettability, surface

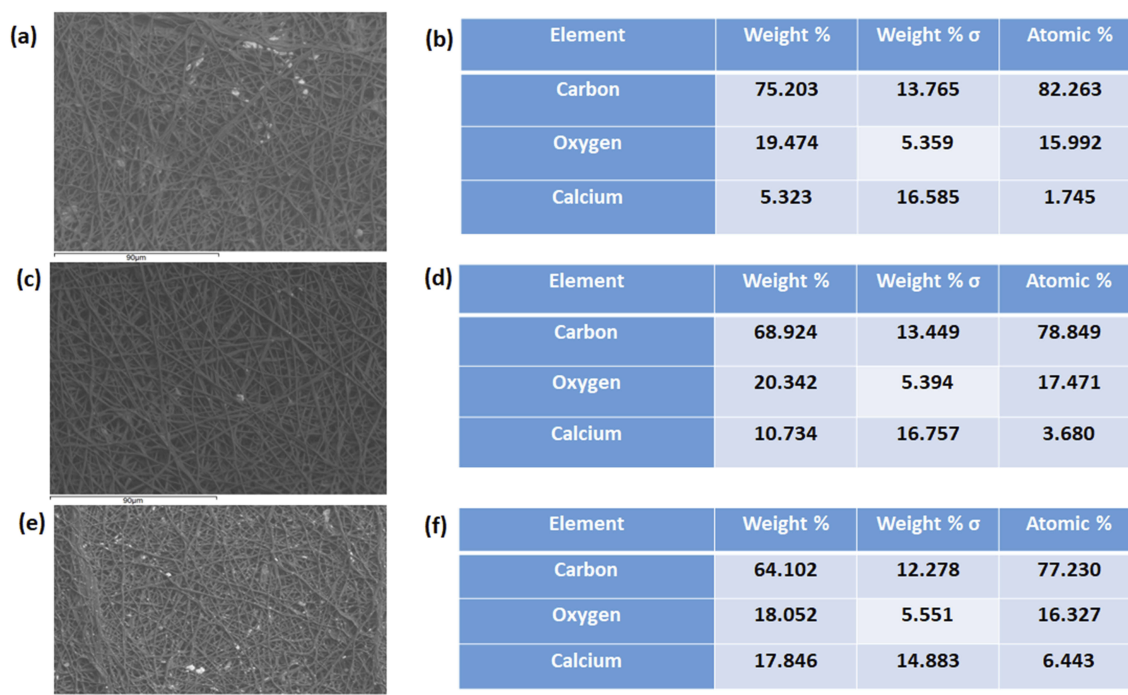


**Figure 8** SEM images of calcium deposition of **(A)** PE, **(C)** PE/WG and **(E)** PE/WG/TiO<sub>2</sub> and EDX graph showing calcium deposition of **(B)** PE, **(D)** PE/WG and **(F)** PE/WG/TiO<sub>2</sub>. Samples (1 \* 1 cm<sup>2</sup>) left in 1.5x SBF (pH 7.4; 37°C) for 14 days was imaged in Hitachi Tabletop TM3000.

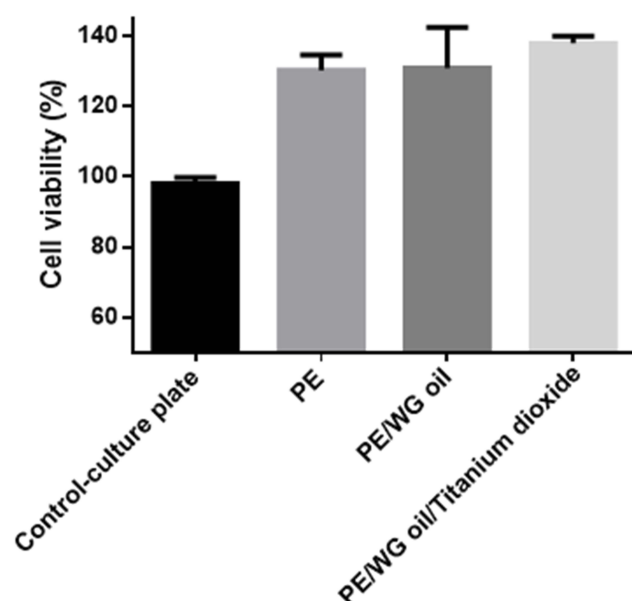


**Figure 9** MTS assay of PE, PE/WG and PE/WG/TiO<sub>2</sub>. Samples with size of 0.5 cm \* 0.5 cm were cut and placed in the 96 well plates. The scaffold was seeded with fibroblast cells with  $10 \times 10^3$  cells/cm<sup>2</sup> density and cultured for 5 days. After 5 days, the medium was added with 20% of MTS reagent for 4 h and optical density (OD) was measured at 490 nm.

roughness, surface chemistry and surface energy.<sup>16,40–43</sup> It has been reported that the smaller fibre diameter,<sup>16</sup> hydrophilic nature<sup>40</sup> and smoother roughness<sup>41</sup> will result in improved cell adhesion and proliferation. The addition of WG and titanium oxide into the PE matrix showed smaller fibre diameter and smoother surfaces which resulted in the improved cellular viability. The periosteum in the human bone is divided into two layer namely the fibrous outer layer and the inner layer is cambium. The fibrous layer is composed of fibroblasts, while the cambium layer has progenitor cells that grow into osteoblasts.<sup>44</sup> Since our fabricated composites showed non-toxic behaviour to the fibroblast cells, it indicated the suitability for the growth of periosteum tissue.

## Conclusion

A novel bone scaffold comprising PE, WG and TiO<sub>2</sub> was manufactured through single-stage electrospinning. Fabricated scaffold displayed improved wettability and thermal properties. Altered surface roughness and improved physicochemical properties resulted in the desirable anticoagulant nature. Enhanced calcium deposition and fibroblast proliferation indicated its suitability for bone tissue engineering. In the future, it would be interesting to investigate the compression testing as well as morphological studies using osteoblast cells for longer

time points which would facilitate this candidate usage in bone tissue engineering.

## Acknowledgments

This work was supported by the Ministry of Higher Education Malaysia with the Grant no. Q.J130000.2545.17H00 and Q.J130000.2545.20H00.

## Disclosure

The authors report no conflicts of interest in this work.

## References

1. Ma PX, Elisseeff J. *Scaffolding in Tissue Engineering*. Boca Raton: Taylor & Francis; 2005.
2. Patrick CW, Mikos AG, McIntire LV. *Frontiers in Tissue Engineering*. 1st ed. Oxford and New York, NY: Pergamon; 1998.
3. Linh NT, Lee BT. Electrospinning of polyvinyl alcohol/gelatin nanofiber composites and cross-linking for bone tissue engineering application. *J Biomater Appl*. 2012;27(3):255–266. doi:10.1177/0885328211401932
4. Dhandayuthapani B, Yoshida Y, Maekawa T, Kumar DS. Polymeric scaffolds in tissue engineering application: a review. *Int J Polym Sci*. 2011;2011:1–19.
5. Huang ZM, Zhang YZ, Kotaki M, Ramakrishna S. A review on polymer nanofibers by electrospinning and their applications in nanocomposites. *Compos Sci Technol*. 2003;63(15):2223–2253. doi:10.1016/S0266-3538(03)00178-7
6. Lyu S, Huang C, Yang H, Zhang X. Electrospun fibers as a scaffolding platform for bone tissue repair. *J Orthopaedic Res*. 2013;31(9):1382–1389. doi:10.1002/jor.22367
7. Bhattarai R, Bachu R, Boddu S, Bhaduri S. Biomedical applications of electrospun nanofibers: drug and nanoparticle delivery. *Pharm*. 2019;11(1):5.
8. Rujitanaroj P, Pimpha N and Supaphol P. Wound-dressing materials with antibacterial activity from electrospun gelatin fiber mats containing silver nanoparticles. *Polym*. 2008;49:4723–4732. doi:10.1016/j.polymer.2008.08.021
9. Bader R, Herzog K, Kao W. A study of diffusion in poly(ethyleneglycol)-gelatin based semi-interpenetrating networks for use in wound healing. *Polym Bull*. 2009;62:381–389. doi:10.1007/s00289-008-0023-x
10. Barhate RS, Ramakrishna S. Nanofibrous filtering media: filtration problems and solutions from tiny materials. *J Membr Sci*. 2007;296:1–8. doi:10.1016/j.memsci.2007.03.038
11. Sill TJ, von Recum HA. Electrospinning: applications in drug delivery and tissue engineering. *Biomater*. 2008;29:1989–2006. doi:10.1016/j.biomaterials.2008.01.011
12. Krishna Rao KSV, Subha MCS, Sairam M, Mallikarjuna NN, Aminabhavi TM. Blend membranes of chitosan and poly(vinyl alcohol) in pervaporation dehydration of isopropanol and tetrahydrofuran. *J Appl Polym Sci*. 2007;103:1918–1926. doi:10.1002/(ISSN)1097-4628
13. John MJ, Thomas S. Biofibres and biocomposites. *Carbohydr Polym*. 2008;71:343–364.
14. Polymer Properties Database. Available from: <https://polymerdatabase.com/polymer%20classes/Polyurethane%20type.html>. Accessed September 17, 2019.
15. Shen Z, Lu D, Li Q, Zhang Z, Zhu Y. Synthesis and characterization of biodegradable polyurethane for hypopharyngeal tissue engineering. *Biomed Res Int*. 2015;2015.
16. Unnithan AR, Pichiah PT, Gnanasekaran G, et al. Emu oil-based electrospun nanofibrous scaffolds for wound skin tissue engineering. *Colloids Surf A Physicochem Eng Asp*. 2012;415:454–460. doi:10.1016/j.colsurfa.2012.09.029

17. Tetteh G, Khan AS, Delaine-Smith RM, Reilly GC, Rehman IU. Electrospun polyurethane/hydroxyapatite bioactive Scaffolds for bone tissue engineering: the role of solvent and hydroxyapatite particles. *J Mech Behavior Biomed Mater*. 2014;39:95–110. doi:10.1016/j.jmbbm.2014.06.019
18. Jing X, Mi HY, Salick MR, Cordie TM, Peng XF, Turng LS. Electrospinning thermoplastic polyurethane/graphene oxide scaffolds for small diameter vascular graft applications. *Mater Sci Eng: C*. 2015;49:40–50. doi:10.1016/j.msec.2014.12.060
19. De Witte TM, Fratila-Apachitei LE, Zadpoor AA, Peppas NA. Bone tissue engineering via growth factor delivery: from scaffolds to complex matrices. *Regener Biomater*. 2018;5(4):197–211. doi:10.1093/rb/rby013
20. Amini AR, Laurencin CT, Nukavarapu SP. Bone tissue engineering: recent advances and challenges. *Crit Rev Biomed Eng*. 2012;40(5):363–408.
21. Jaganathan SK, Mani MP, Nageswaran G, Krishnasamy NP, Ayyar M. Single stage electrospun multicomponent scaffold for bone tissue engineering application. *Polym Test*. 2018;70:244–254. doi:10.1016/j.polymertesting.2018.07.015
22. De Silva RT, Mantilaka MM, Goh KL, Ratnayake SP, Amarantunga GA, de Silva KM. Magnesium oxide nanoparticles reinforced electrospun alginate-based nanofibrous scaffolds with improved physical properties. *Int J Biomater*. 2017;2017.
23. Rodríguez-Tobías H, Morales G, Ledezma A, Romero J, Grande D. Novel antibacterial electrospun mats based on poly (d, l-lactide) nanofibers and zinc oxide nanoparticles. *J Mater Sci*. 2014;49(24):8373–8385. doi:10.1007/s10853-014-8547-y
24. Ali B, Al-Wabel NA, Shams S, Ahamad A, Khan SA, Anwar F. Essential oils used in aromatherapy: a systemic review. *Asian Pac J Trop Biomed*. 2015;5(8):601–611. doi:10.1016/j.apjtb.2015.05.007
25. Nikolić M, Marković T, Mojović M, et al. Chemical composition and biological activity of *Gaultheria procumbens* L. essential oil. *Indus Crop Prod*. 2013;49:561–567. doi:10.1016/j.indcrop.2013.06.002
26. Facciola S. *Cornucopia II: A Source Book of Edible Plants*. 2nd ed. UK: Kampong Publications; 1998.
27. Genders R. *Scented Flora Of the World. R. Halle Illustrated*. Pennsylvania State University; 1977.
28. Wang X, Zhu J, Yin L, et al. Evaluation of the morphology and osteogenic potential of titania-based electrospun nanofibers. *J Nanomater*. 2012;2012:20. doi:10.1155/2012/959578
29. Adhikari SP, Pant HR, Mousa HM, et al. Synthesis of high porous electrospun hollow TiO<sub>2</sub> nanofibers for bone tissue engineering application. *J Indus Eng Chem*. 2016;35:75–82. doi:10.1016/j.jiec.2015.12.004
30. Balaji A, Jaganathan SK, Ismail AF, Rajasekar R. Fabrication and hemocompatibility assessment of novel polyurethane-based bio-nanofibrous dressing loaded with honey and carica papaya extract for the management of burn injuries. *Int J Nanomedicine*. 2016;11:4339. doi:10.2147/IJN.S112265
31. Mani MP, Jaganathan SK. Fabrication and characterization of electrospun polyurethane blended with dietary grapes for skin tissue engineering. *J Indus Text*. 2019;1528083719840628.
32. Jaganathan SK, Mani MP, Ayyar M, Krishnasamy NP, Nageswaran G. Blood compatibility and physicochemical assessment of novel nanocomposite comprising polyurethane and dietary carotino oil for cardiac tissue engineering applications. *J Appl Polym Sci*. 2018;135(3):45691. doi:10.1002/app.45691
33. Manikandan A, Mani MP, Jaganathan SK, Rajasekar R. Morphological, thermal, and blood-compatible properties of electrospun nanocomposites for tissue engineering application. *Polym Compos*. 2018;39:E132–E139. doi:10.1002/pc.v39.S1
34. Theivasanthi T, Alagar M. Titanium dioxide (TiO<sub>2</sub>) nanoparticles XRD analyses: an insight. 2013. arXiv:1307.1091.
35. Jaganathan SK, Mani MP. Electrospun polyurethane nanofibrous composite impregnated with metallic copper for wound-healing application. *3 Biotech*. 2018;8(8):327. doi:10.1007/s13205-018-1356-2
36. Jaganathan SK, Mani MP, Palaniappan SK, Rathanasamy R. Fabrication and characterisation of nanofibrous polyurethane scaffold incorporated with corn and neem oil using single stage electrospinning technique for bone tissue engineering applications. *J Polym Res*. 2018;25(7):146. doi:10.1007/s10965-018-1543-1
37. Kim HH, Kim MJ, Ryu SJ, Ki CS, Park YH. Effect of fiber diameter on surface morphology, mechanical property, and cell behavior of electrospun poly (ε-caprolactone) mat. *Fiber Polym*. 2016;17(7):1033–1042. doi:10.1007/s12221-016-6350-x
38. Ribeiro C, Sencadas V, Areias AC, Gama FM, Lanceros-Méndez S. Surface roughness dependent osteoblast and fibroblast response on poly (l-lactide) films and electrospun membranes. *J Biomed Mater Res Part A*. 2015;103(7):2260–2268. doi:10.1002/jbm.a.35367
39. Mani MP, Jaganathan SK, Khudzari AZ, Rathanasamy R, Prabhakaran P. Single-stage electrospun innovative combination of polyurethane and neem oil: synthesis, characterization and appraisal of blood compatibility. *J Bioact Compat Polym*. 2018;33(6):573–584. doi:10.1177/0883911518792288
40. Miguel SP, Ribeiro MP, Coutinho P, Correia IJ. Electrospun polycaprolactone/aloe vera chitosan nanofibrous asymmetric membranes aimed for wound healing applications. *Polymers*. 2017;9(5):Article 183. doi:10.3390/polym9120669
41. Chou SH, Don TM, Lai WC, Cheng LP. Formation of microporous poly (hydroxybutyric acid) membranes for culture of osteoblast and fibroblast. *Polym Adv Technol*. 2009;20(12):1082–1090. doi:10.1002/pat.1366
42. Anselme K, Ploux L, Ponche A. Cell/material interfaces: influence of surface chemistry and surface topography on cell adhesion. *J Adhes Sci Technol*. 2010;24(5):831–852. doi:10.1163/016942409X12598231568186
43. Hallab NJ, Bundy KJ, O'Connor K, Moses RL, Jacobs JJ. Evaluation of metallic and polymeric biomaterial surface energy and surface roughness characteristics for directed cell adhesion. *Tissue Eng*. 2001;7(1):55–71. doi:10.1089/107632700300003297
44. Periosteum. Available from: <https://en.wikipedia.org/wiki/Periosteum>. Accessed 6th August 2019.

## International Journal of Nanomedicine

### Publish your work in this journal

The International Journal of Nanomedicine is an international, peer-reviewed journal focusing on the application of nanotechnology in diagnostics, therapeutics, and drug delivery systems throughout the biomedical field. This journal is indexed on PubMed Central, MedLine, CAS, SciSearch®, Current Contents®/Clinical Medicine,

Submit your manuscript here: <https://www.dovepress.com/international-journal-of-nanomedicine-journal>

Dovepress

Journal Citation Reports/Science Edition, EMBASE, Scopus and the Elsevier Bibliographic databases. The manuscript management system is completely online and includes a very quick and fair peer-review system, which is all easy to use. Visit <http://www.dovepress.com/testimonials.php> to read real quotes from published authors.